Smart Mater. Struct. 2 (1993) 22–30. Printed in the UK

Carbon fiber reinforced concrete for smart structures capable of non-destructive flaw detection

Pu-Woei Chen and D D L Chung
Department of Mechanical and Aerospace Engineering, State University of New York at Buffalo, Box 604400, Buffalo, NY 14260–4400, USA

Received 30 November 1992, accepted for publication 18 January 1993

Abstract. Electrically conducting concrete, as provided by the addition of short carbon fibers (0.2–0.4 vol. %) to concrete, can function as a smart structure material that allows non-destructive electrical probing for the monitoring of flaws. The electrical signal is related to an increase in the concrete's volume resistivity during crack generation or propagation and a decrease in the resistivity during crack closure. The linearity between the volume resistivity change and the compressive stress was good for mortar containing carbon fibers together with either methylcellulose or latex as dispersants. However, the linearity was poor for mortar containing carbon fibers together with both methylcellulose and silica fume, as this mortar required a minimum compressive stress for crack closure, whereas the other two mortars did not. When the compressive stress was increased in the first cycle up to the fracture stress, the volume resistivity increased by 1040 % for the mortar containing carbon fibers and methylcellulose, but only 385 % for that containing fibers and latex. In contrast, mortars without carbon fibers showed no variation of the resistivity upon compression up to fracture.

1. Introduction

Smart concrete structures that provide the capability of non-destructive flaw detection allow concrete structures to be repaired before it is too late. This capability is critically needed for highways, bridges and nuclear power plants. This paper describes electrically conducting concrete (made conducting by the addition of carbon fibers) for use as an intrinsically smart structure material that is capable of non-destructive flaw detection. This capability is based on the notion that the volume electrical resistivity of electrically conducting concrete increases upon flaw generation or propagation.

No works on intrinsically smart concrete have been previously published except for a 1992 news article (*ENG* June 22 pp 14–15) on 'self-test concrete' involving glass and carbon fibers and developed by H Yanagida of the University of Tokyo. Most prior work relates to concrete rendered smart extrinsically by the use of embedded sensors or an embedded chemical. The embedded chemical (calcium nitrite contained in polypropylene fibers) is for anticorrosion of steel reinforcement bars; the technology was developed by C Dry of University of Illinois, Urbana, and disclosed in another 1992 news article (Stuat T 1992 *R & D magazine* pp 74–8). An intrinsically smart concrete is more versatile and more convenient to use than an extrinsically smart concrete. In particular, the carbon fibers in carbon fiber reinforced concrete serve to provide the smart action as well as improved structural performance. Furthermore, the addition of carbon fibers to concrete can be achieved by simply using the conventional stone concrete mixer.

The addition of carbon fibers to concrete had been previously found to increase the flexural strength, flexural toughness [1–11] and freeze–thaw durability [1], and to decrease the drying shrinkage [1] and the electrical resistivity [1, 2]. Effective use of the fibers requires fiber dispersion, which is enhanced by the addition of methylcellulose [1], latex [2] or silica fume [1–11].

2. Experimental details

2.1. Raw materials

The short carbon fibers were isotropic pitch based and unsized. The nominal fiber length was 5.1 mm. The fiber properties are shown in table 1. Fibers in the amount of 0.5 % by weight of cement were used. The aggregate used was natural sand, the particle size analysis of which is shown in figure 1. Table 2 describes the various raw materials used. Table 3 describes the four types of mortar studied. They are (i) plain mortar, (ii) plain mortar with

0964-1726/93/010022 + 09 $07.50

Table 1. Properties of carbon fibers.

Filament diameter	10 μm
Tensile strength	690 MPa
Tensile modulus	48 GPa
Elongation at break	1.4%
Electrical resistivity	3.0×10^{-3} Ωcm
Specific gravity	1.6 g cm^{-3}
Carbon content	98 wt.%

latex, (iii) plain mortar with methylcellulose and (iv) plain mortar with methylcellulose and silica fume. The latex, methylcellulose and silica fume were added to disperse the fibers, but in each category such additives were used whether fibers were present or not in order to obtain the effect of the fiber addition alone. In addition, latex and silica fume served to enhance the fiber–matrix bonding.

The water reducing agent powder used was TAMOL SN (Rohm and Haas) which contained 93–96 % sodium salt of a condensed naphthalenesulfonic acid. In general, the slump of carbon fiber reinforced cement tends to decrease with increasing carbon fiber content. Therefore, we used various amounts of this water reducing agent in order to maintain the mortar at a reasonable flow value in the range of 150 $\pm$ 50 mm.

The latex was a styrene butadiene polymer emulsion; it was used in the amount of 20 % of the weight of the cement. The antifoam (Dow Corning 2410, an emulsion) used was in the amount of 0.5 % of the weight of the latex; it was used whenever latex was used.

Methylcellulose in the amount of 0.4 % of the cement weight was used. The defoamer (Colloids 1010) used along with it was in the amount of 0.13 vol. %; it was used whenever methylcellulose was used.

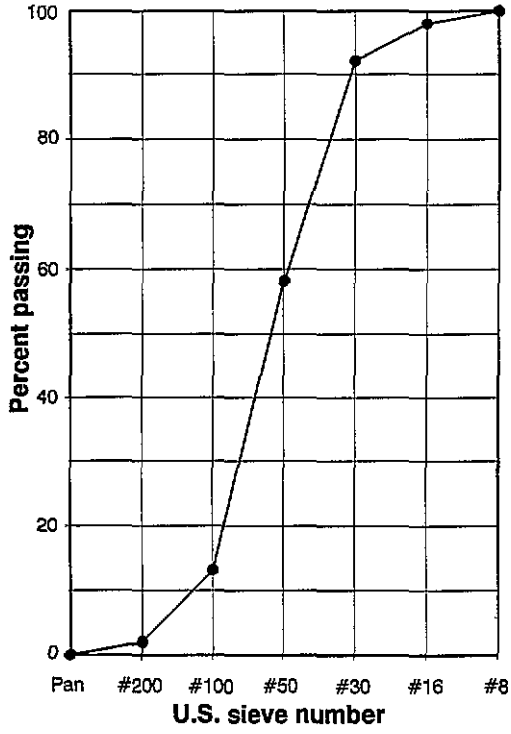

Figure 1. Particle size distribution of the sand used.

2.2. Mixing procedure

A Hobart mixer with a flat beater was used for mixing.

For the case of mortar containing latex, the latex, antifoam and carbon fibers first were mixed by hand for about 1 min. Then this mixture, cement, sand, water and the water reducing agent were mixed in the Hobart mixer for 5 min.

For the case of mortar containing methylcellulose, methylcellulose was dissolved in water and then fibers and the defoamer were added and stirred by hand for about 2 min. Then this mixture, cement, sand, water and water reducing agent (and silica fume, if applicable) were mixed in the Hobart mixer for 5 min.

After pouring the mix into oiled molds, a vibrator was used to decrease the amount of air bubbles.

2.3. Curing procedure

The specimens were demolded after 1 d and then allowed to cure at room temperature in air for 7 d.

2.4. Testing procedure

According to ASTM C109–80, specimens were prepared by using a 2 × 2 × 2 in (5.1 × 5.1 × 5.1 cm) mold for compressive testing. Compression testing was performed using a hydraulic Material Testing System (MTS). During cyclic compressive loading and unloading, the volume electrical resistivity was measured along the stress axis, using the four-probe method. Electrical contacts were made by silver paint applied along the whole perimeter in four parallel planes perpendicular to the stress axis. The inner two contacts were for voltage measurement, while the outer two contacts were for passing a current. Although the spacing between the contacts decreased upon compressive deformation, the decrease was so small that the measured resistance remained proportional to the volume resistivity. Testing was performed either in one cycle up to the breaking stress or in multiple cycles upon loading up to a compressive stress equal to a fraction ($\frac{1}{5}$, $\frac{1}{4}$, $\frac{1}{3}$ or $\frac{1}{2}$) of the breaking stress. Unless stated otherwise, this fraction was $\frac{1}{3}$.

2.5. Results

Figures 2–8 show the compressive stress and volume electrical resistivity during loading in one cycle up to the fracture stress for the seven mortars listed in table 3. All mortars without fibers (figures 2, 3, 5 and 7) showed no or negligible change in the resistivity upon compression up to fracture. However, all mortars with fibers (figures 4, 6 and 8) showed increasing resistivity upon compression up to fracture. For the case of figure 8 (mortar with fibers, methylcellulose and silica fume), the resistivity increase was gradual at compressive stresses below about 0.75 of the fracture stress and was abrupt and quite linear versus stress at stresses above this value. In the case of figure 4 (mortar with fibers and latex), the resistivity did

Table 2. List of raw materials.

Material	Source
Portland cement Type I	Lafarge Corporation (Southfield, MI)
TAMOL SN Sodium salt of a condensed naphthalenesulfonic acid (93–96%) Water (51–54%)	Rohm and Haas Company (Philadelphia, PA)
Methocel, A15-LV Methylcellulose	Dow Chemical Corporation (Midland, MI)
Colloids 1010 Defoamer	Colloids Inc. (Marietta, GA)
Latex 460NA Styrene butadiene (40–60%) Water (40–60%) Stabilizer (1–5%)	Dow Chemical Corporation (Midland, MI)
Antifoam 2410 Polydimethylsiloxane (10%) Water, preservatives and emulsifiers (90%)	Dow Corning Corporation (Midland, MI)
Silica fume	Elkem Materials Inc. (Pittsburgh, PA)
Carboflex Carbon fibers	Ashland Petroleum Company (Ashland, KY)

not start to increase until the compressive stress had reached about 0.68 of the fracture stress. In the case of figure 6 (mortar with fibers and methylcellulose), the resistivity increase was gradual at compressive stresses below about 0.13 of the fracture stress and was abrupt and quite linear versus stress at stresses above this value. The fractional increase in resistivity from zero stress to the fracture stress was 385 %, 1040 % and 1660 % for figures 4, 6 and 8 respectively. Thus, among the three fiber-containing mortars, the one with methylcellulose (figure 6) was most attractive, as it exhibited a combination of linearity (between resistivity and stress) and large fractional resistivity increase. The exceptionally low value of the fractional resistivity increase for the mortar with fibers and latex (figure 4) is attributed to the large amount of latex (20 % of the cement weight) compared to the small amount of methylcellulose (0.4 % of the cement weight) and also to the electrically insulating property of latex, which is a polymer. Note that the resistivity itself was higher for the mortar containing fibers and latex than the other two fiber-containing mortars.

For all mortars with fibers (figures 4, 6 and 8), the apparent resistivity decreased when the mortar fractured; this is because of the collapse of the mortar, thus bringing together the originally dispersed fibers. For all mortars without fibers (figures 2, 3, 5 and 7), the resistivity increased abruptly when the mortar fractured; this is because of the widespread cracking which accompanied fracture and the fact that the mortar was more conductive than air.

Figure 9 shows the variation of the compressive stress

Table 3. Mix proportions of four types of mortar.

Sample	Fiber vol.%	Water/cement ratio	Sand/cement ratio	Latex/cement ratio	Meth/cement (%)	SF/cement ratio	WR/cement (%)
Plain mortar	0	0.45	1.5	–	–	–	–
Plain mortar	0	0.3	1.0	0.2	–	–	–
with latex	0.37	0.3	1.0	0.2	–	–	–
Plain mortar	0	0.45	1.5	–	0.4	–	–
with Meth	0.24	0.45	1.5	–	0.4	–	2
Plain mortar	0	0.45	1.5	–	0.4	0.15	2
with Meth and silica fume	0.24	0.45	1.5	–	0.4	0.15	2

Meth = methylcellulose
SF = silica fume
WR = water reducing agent.

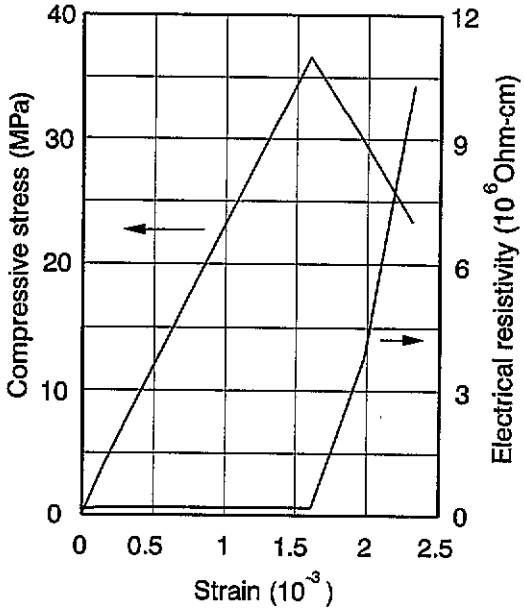

Figure 2. Compressive stress and electrical resistivity versus strain curves for plain mortar.

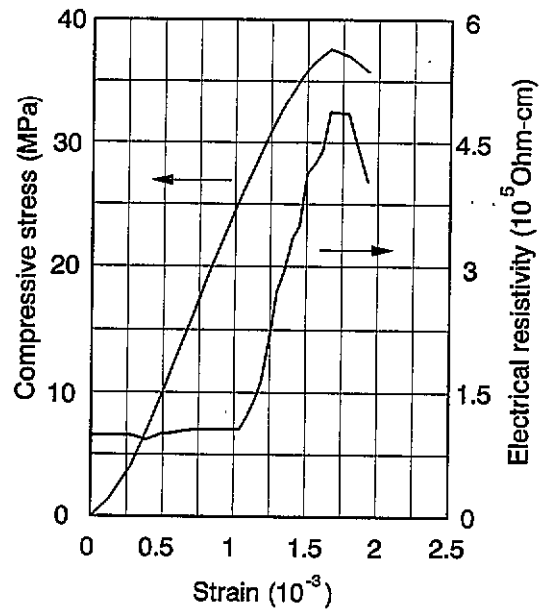

Figure 4. Compressive stress and electrical resistivity versus strain curves for plain mortar containing latex and 0.37 vol. % carbon fibers.

and strain during the first three loading cycles carried out to a compressive stress equal to about $\frac{1}{3}$ of the fracture stress. The same maximum stress was used for all seven mortars of table 3. The variation of the resistivity during these three cycles is shown in figures 10–16 for these seven mortars. All mortars without fibers (figures 10, 11, 13 and 15) showed no change in the resistivity during the stress cycling. All mortars with fibers (figures 12, 14, and 16) showed (i) irreversibly increasing resistivity during the first loading, (ii) reversibly increasing resistivity during unloading in any cycle, and (iii) reversibly decreasing resistivity during the second and subsequent loadings.

The irreversibly increasing resistivity during the first loading is attributed to flaw generation. The reversibly increasing resistivity during unloading in any cycle is attributed to crack opening, which was hindered under compressive loading. The reversibly decreasing resistivity during the second and subsequent loadings is attributed to the crack closure under compressive loading. The onset of the resistivity decrease during loading in the second and subsequent cycles occurred at a compressive stress of 0, 0 and 0.57 of the maximum stress for the mortar with fibers and latex (figure 12), the mortar with fibers and methylcellulose (figure 14) and the mortar with

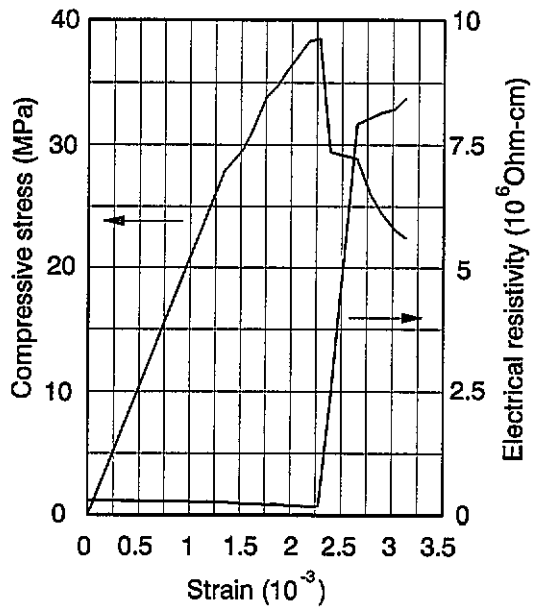

Figure 3. Compressive stress and electrical resistivity versus strain curves for plain mortar containing latex.

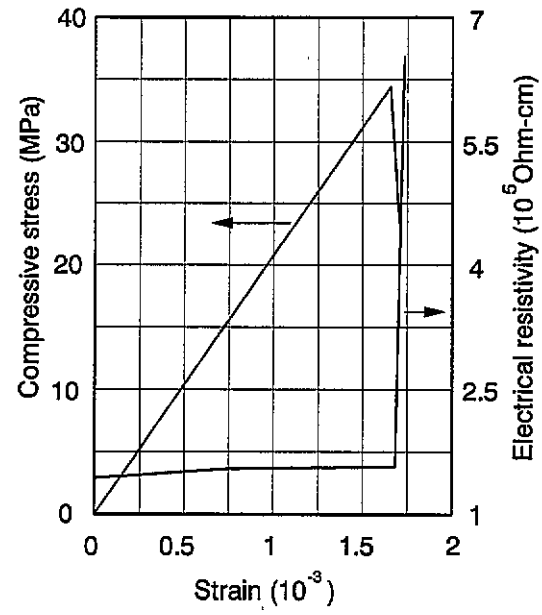

Figure 5. Compressive stress and electrical resistivity versus strain curves for mortar containing methylcellulose.

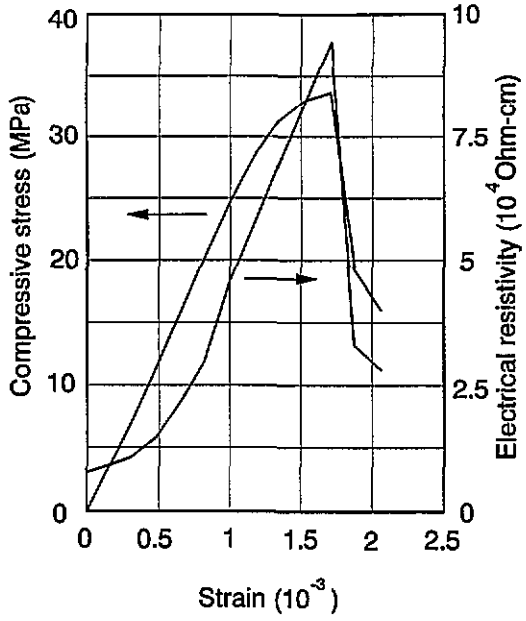

Figure 6. Compressive stress and electrical resistivity versus strain curves for mortar containing methylcellulose and 0.24 vol. % carbon fibers.

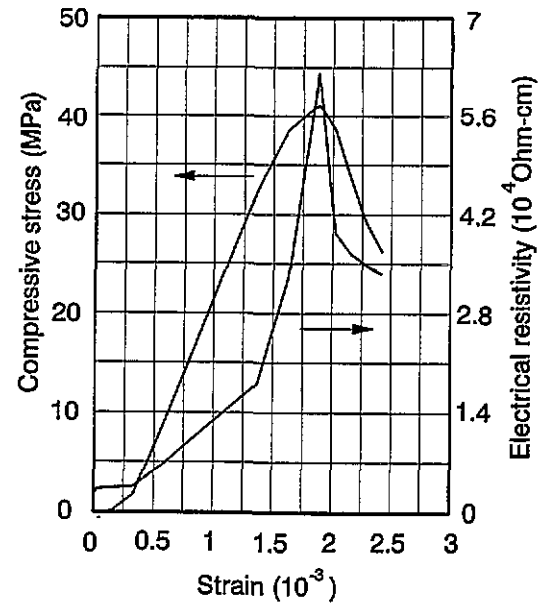

Figure 8. Compressive stress and electrical resistivity versus strain curves for mortar containing methylcellulose, silica fume and 0.24 vol. % carbon fibers.

fibers, methylcellulose and silica fume (figure 16), respectively. The fractional decrease in the resistivity upon loading in the second and subsequent cycles was 33 %, 27 % and 32 % for the mortar with fibers and latex (figure 12), the mortar with fibers and methylcellulose (figure 14) and the mortar with fibers, methylcellulose and silica fume (figure 16), respectively. The roughly linear behavior of the resistivity decrease (versus stress) for the mortar with fibers and latex (figure 12) and the mortar with fibers and methylcellulose (figure 14) indicates that these two mortars can be used as smart structure materials that are capable of non-destructive monitoring of cracking.

The mortar containing fibers and latex was the most expensive among the seven mortars studied because of the cost of the large amount of latex used. Thus, with economy in mind, it can be concluded that the mortar containing fibers and methylcellulose is the most attractive among the seven mortars for use as a smart structure material.

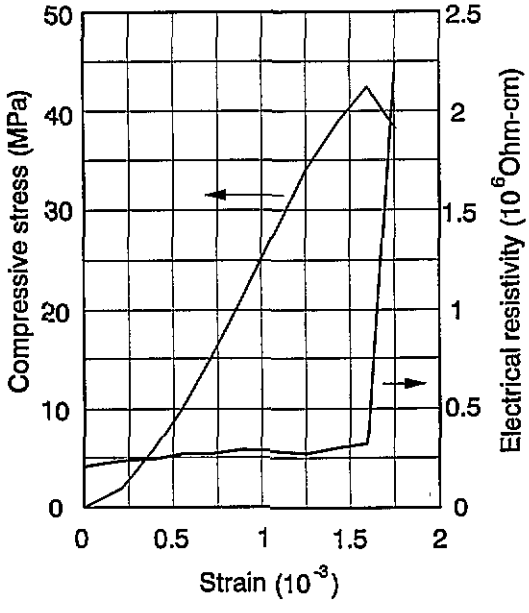

Figure 7. Compressive stress and electrical resistivity versus strain curves for mortar containing methylcellulose and silica fume.

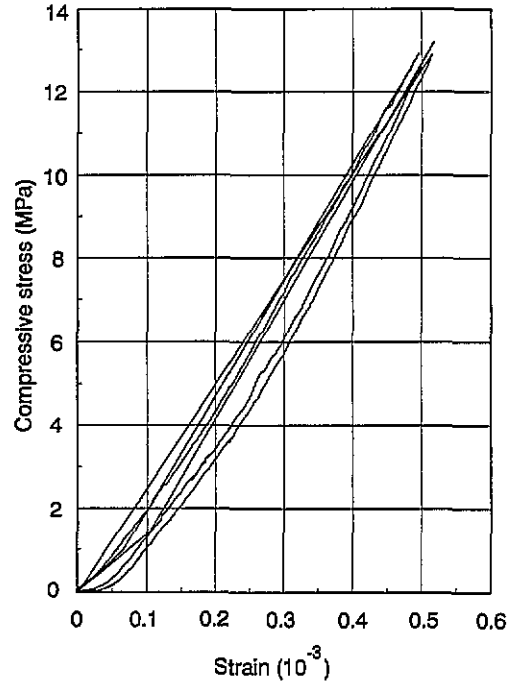

Figure 9. Compressive stress versus strain curves for cyclic loading and simultaneous electrical resistivity testing.

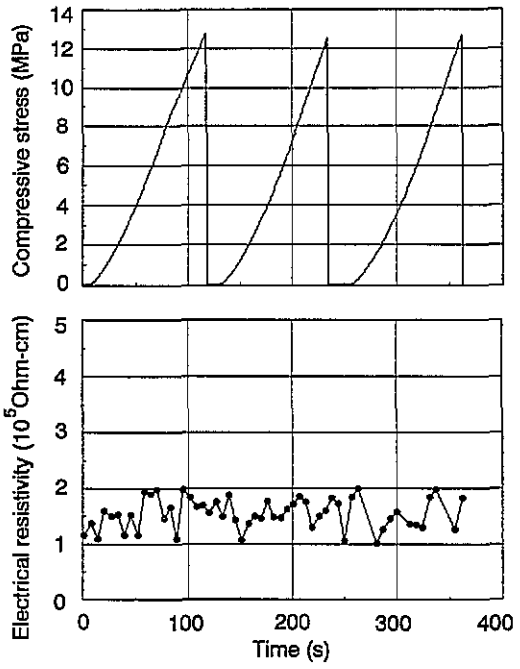

Figure 10. Cyclic compressive stress and electrical resistivity versus time curves for plain mortar.

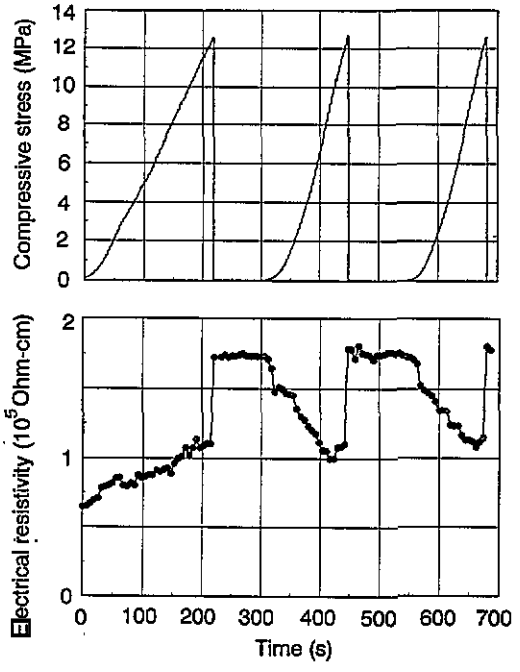

Figure 12. Cyclic compressive stress and electrical resistivity versus time curves for mortar containing latex and 0.37 vol. % carbon fibers.

Figure 17 shows results similar to those in figure 12 and for the same mortar (with latex and fibers) as figure 12, but for a maximum compressive stress equal to $\frac{1}{5}$ (rather than $\frac{1}{3}$) of the breaking stress. The change in the resistivity during stress cycling was only $0.01 \times 10^5\ \Omega$cm for a maximum stress of $\frac{1}{5}$ of the breaking stress (figure 17), compared to a value of $0.7 \times 10^5\ \Omega$cm for a maximum stress of $\frac{1}{3}$ of the breaking stress (figure 12). It is significant that the electrical signal was detectable even at a low maximum stress of $\frac{1}{5}$ of the breaking stress.

Figure 18 shows the correlation of the maximum stress with the flaw structure, as observed by scanning election microscopy (SEM) after stress cycling for a cut (SiC wheel) section parallel to the stress direction. All the samples in figure 18 were mortar containing latex and

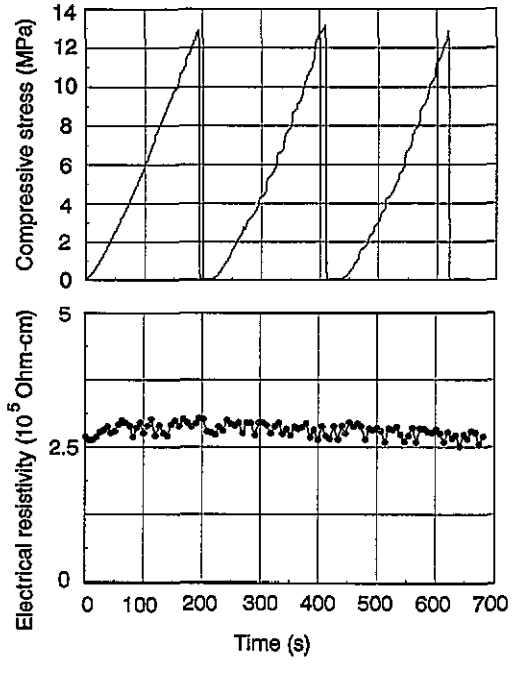

Figure 11. Cyclic compressive stress and electrical resistivity versus time curves for mortar containing latex.

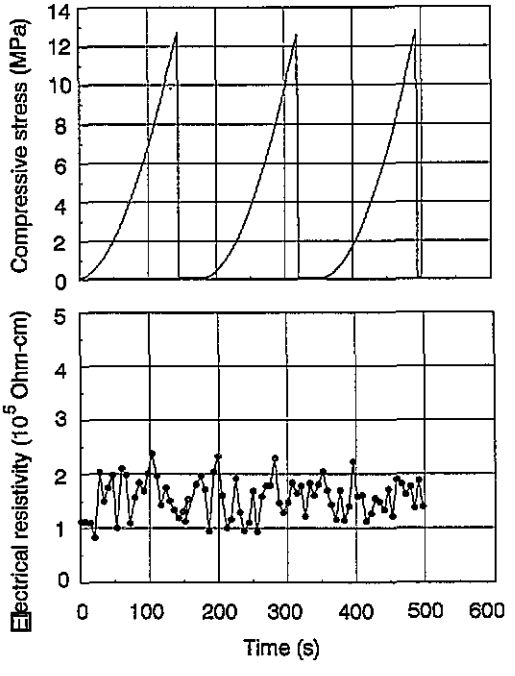

Figure 13. Cyclic compressive stress and electrical resistivity versus time curves for mortar containing methylcellulose.

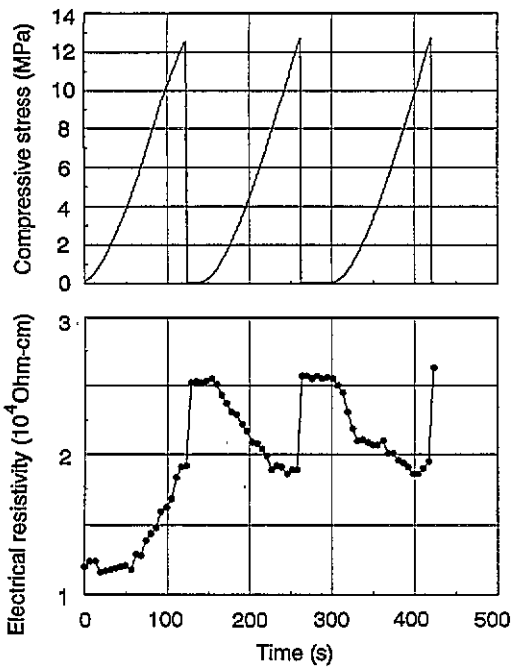

Figure 14. Cyclic compressive stress and electrical resistivity versus time curves for mortar containing methylcellulose and 0.24 vol. % carbon fibers.

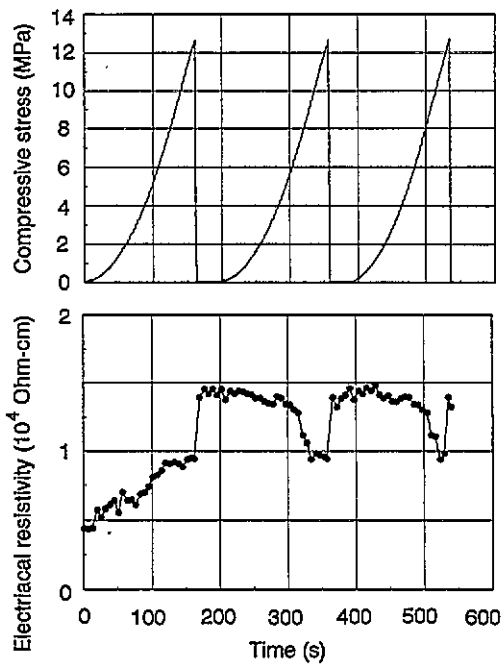

Figure 16. Cyclic compressive stress and electrical resistivity versus time curves for mortar containing methlcellulose, silica fume and 0.24 vol. % carbon fibers.

fibers. The greater was the maximum stress, the larger and more numerous were the cracks.

Preliminary results obtained on concrete (not mortar) containing fibers (0.19 vol. %) and methylcellulose after 7 and 28 days of curing were similar to those of the mortars. Thus, the smart behavior applies to concretes as

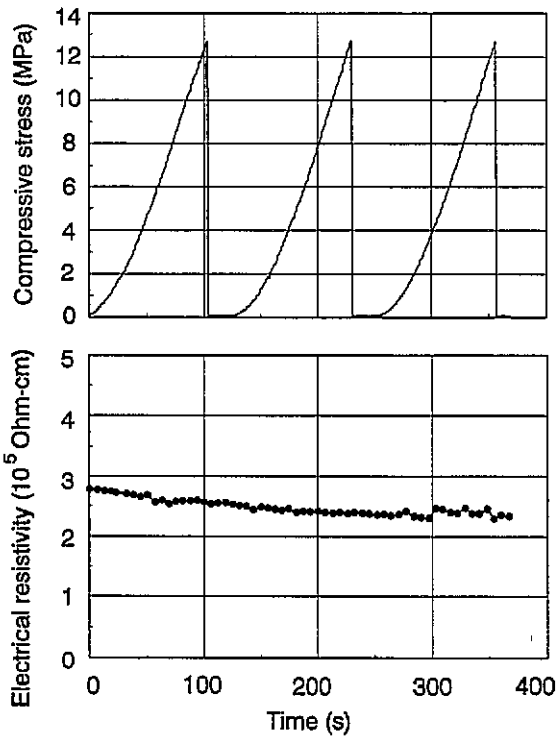

Figure 15. Cyclic compressive stress and electrical resistivity versus time curves for mortar containing methylcellulose and silica fume.

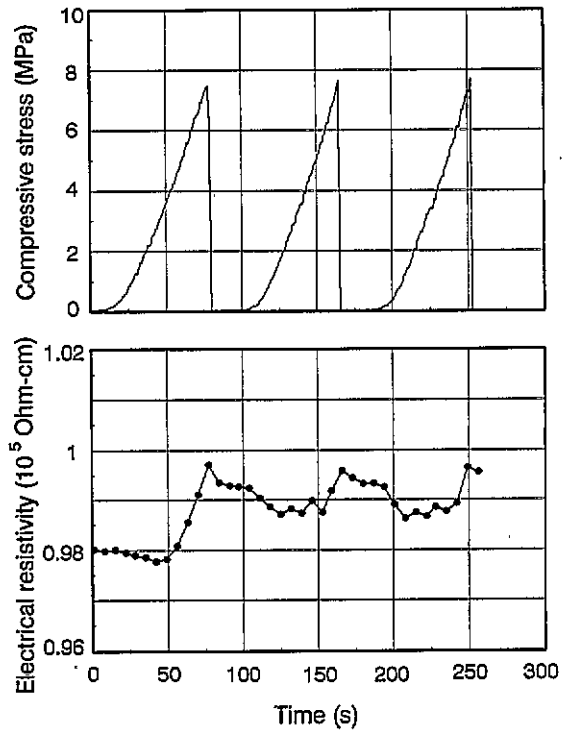

Figure 17. Cyclic compressive stress and electrical resistivity versus time curves for mortar containing latex and 0.37 vol. % carbon fibers. The maximum stress was $\frac{1}{5}$ of the breaking stress.

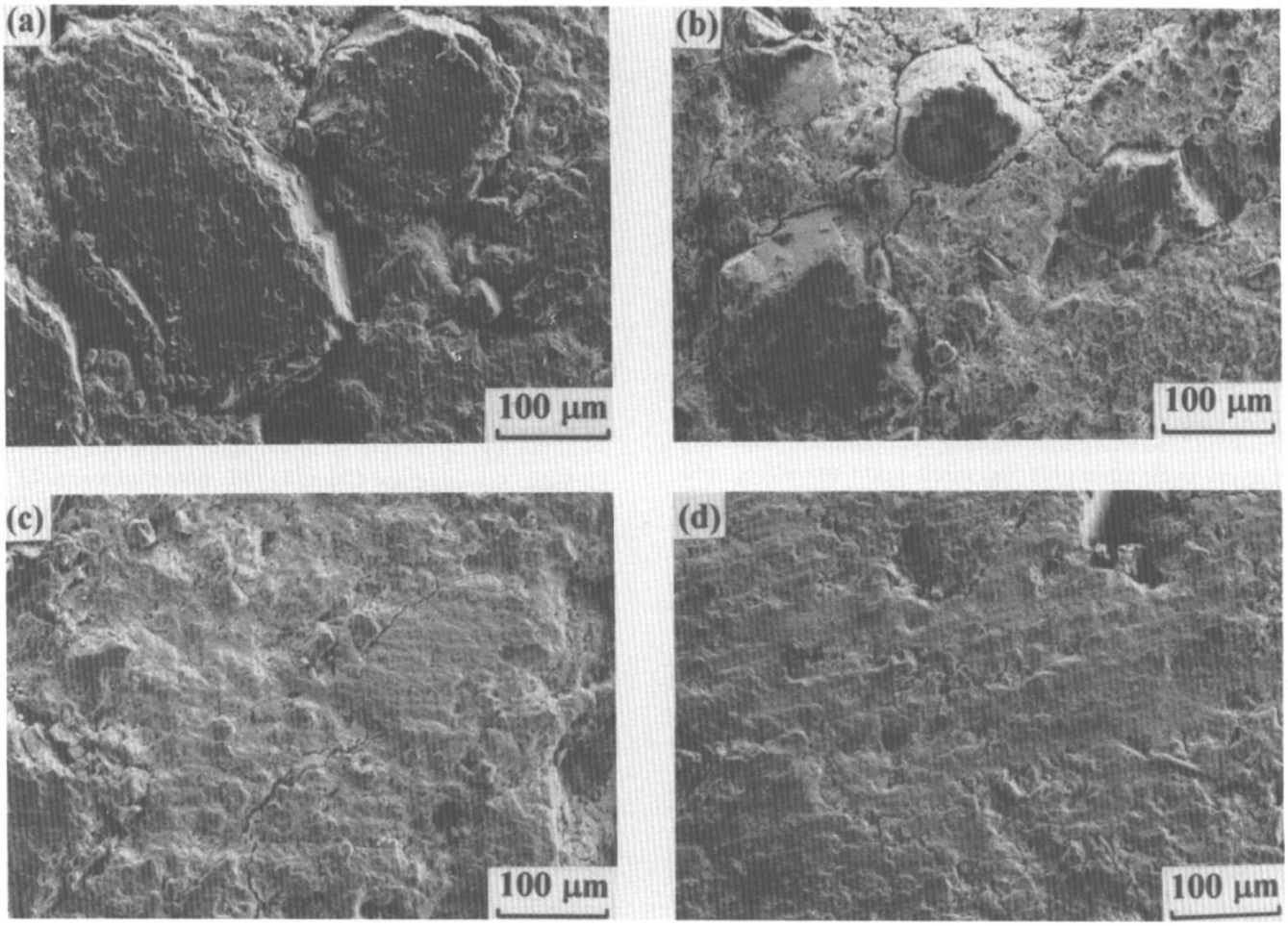

Figure 18. SEM photographs of cut surfaces (along the stress direction) of mortar containing latex and 0.37 vol. % carbon fibers and having been compressed to (*a*) $\frac{1}{2}$ of fracture stress, (*b*) $\frac{1}{3}$ of fracture stress, (*c*) $\frac{1}{4}$ of fracture stress, and (*d*) $\frac{1}{5}$ of fracture stress.

well as mortars. The details of the concrete tested can be found in [1].

3. Discussion

This paper provides a new method for achieving smartness in concrete structures. This method involves the use of electrically conducting concrete as the smart material. By non-destructive electrical probing, flaws in the structure can be detected.

Although this paper used silver paint for the electrical contacts, pressure contacts may be used instead. As shown in a separate paper [3], the pressure needed to achieve a minimum contact resistivity between mortar and steel was 0.00 MPa for carbon fiber reinforced mortar and 0.05 MPa for plain mortar. Furthermore, the contact resistivity between mortar and steel was 10^3–$10^5\ \Omega\,cm^2$ for carbon fiber reinforced mortar and $10^9\ \Omega\,cm^2$ for plain mortar [3]. Thus, simple and inexpensive pressure contacts with a negligible pressure requirement can be used in place of the silver paint contacts.

The shape of the silver paint contacts used in this work was that of a strip going all the way around the mortar. This shape helps maintain an equipotential plane in the plane of the strip. An equipotential plane is needed for quantitative volume resistivity measurement. However, in the field, quantitative volume resistivity measurement is not necessary. For a qualitative measurement of the relative changes in the resistivity, an equipotential plane is not necessary and the shape of the contact does not matter. For example, it can be a point contact.

The four-probe method was used in this work for the resistivity measurement. This method enables the measurement of the volume resistance even in the presence of a non-zero contact resistance, so it is necessary for accurate volume resistivity measurement. However, in the field, quantitative volume resistivity measurement is not necessary, so the four-probe method may be replaced by the two-probe method, if utmost simplicity is desired.

As the electrical probing can be performed at any part of a concrete structure, it can provide information on the flaw distribution in a concrete structure.

Although this work used mortars rather than concretes, similar results can be obtained with carbon fiber reinforced concretes. Carbon fibers are known to decrease

the volume electrical resistivity of both mortars and concretes [1].

The amount of carbon fibers used in this work was only 0.2–0.4 vol. %. This low fiber content is desirable for the sake of materials and processing economy. Although a Hobart mixer was used in the concrete mixing in this work, it can be replaced by a stone concrete mixer [4].

4. Conclusions

The volume electrical resistivity of carbon fiber reinforced concrete was found to increase irreversibly upon increasing compressive loading up to about $\frac{1}{3}$ of the breaking load in the first loading cycle, and subsequently in every cycle reversibly increased upon unloading and reversibly decreased upon loading. This effect is attributed to irreversible flaw generation in the first loading, reversible crack opening in subsequent unloading and reversible crack closure in subsequent loading. In contrast, the resistivity was constant during loading and unloading in any cycle for the case of concrete without fibers. Thus, carbon fiber reinforced concrete can serve as a smart structure material, the volume resistivity of which can be non-destructively monitored to detect flaws. Roughly linear relationships were observed among the volume resistivity change, the compressive stress and the compressive strain in any cycle for mortar containing 0.4 vol. % fibers and latex in the amount of 0.2 of the cement weight, and for mortar containing 0.2 vol. % fibers and methylcellulose in the amount of 0.4 % of the cement weight. Non-linear behavior was observed for mortar containing 0.2 vol. % fibers, methylcellulose in the amount of 0.4 % of the cement weight and silica fume in the amount of 0.15 of the cement weight. The non-linear behavior of the last case was such that a minimum non-zero stress was necessary for crack closure and the resulting resistivity decrease. No such minimum stress was necessary for the first two cases. When the compressive stress was increased in the first cycle up to the fracture stress, the resistivity increased by 1040 % for the mortar containing fibers and methylcellulose, but only 385 % for that containing fibers and latex.

References

[1] Chen Pu-Woei and Chung D D L 1993 *Composites* **24** 33–52

[2] Yang Xiaoming and Chung D D L 1992 *Composites* **23** 453–60

[3] Chen Pu-Woei and Chung D D L 1992 *Smart Mater. Struct.* submitted for publication

[4] Chen Pu-Woei and Chung D D L to be published

[5] Furukawa S, Tsuji Y and Otani S 1987 *Proc. 30th Japan. Congr. of Material Research* pp 149–152

[6] Akihama S, Suenaga T and Banno T 1986 *Int. J. Cement Composites Lightweight Concrete* **8** 21–33

[7] Akihama S, Kobayashi M, Suenaga T, Nakagawa H and Suzuki K 1986 *Kajima Institute of Construction Technology Report 65* October 1986

[8] Ohama Y, Sato Y and Endo M 1986 *Proc. Asia-Pacific Concrete Technology Conf. '86 (Singapore 1986)* pp 5.1–5.8

[9] Park S B and Lee B I 1991 *Proc. 1990 Fall Mater. Res. Soc. Simp. vol 211* pp 247–54

[10] Zheng Q and Chung D D L 1989 *Cement Concrete Res.* **19** 25–41

[11] Larson B K, Drzal L J and Sorousian P 1990 *Composites* **21** 205–15